SUPPORTING INFORMATION

Basic Quinolinonyl Diketo Acid Derivatives as Inhibitors of HIV Integrase and their Activity Against RNase H Function of Reverse Transcriptase

Roberta Costi,[,†] Mathieu Métifiot,[ƒ] Suhman Chung,[⊥] Giuliana Cuzzucoli Crucitti,[†] Kasthuraiah Maddali,[ƒ] Luca Pescatori,[†] Antonella Messore,[†] Valentina Noemi Madia,[†] Giovanni Pupo,[†] Luigi Scipione,[†] Silvano Tortorella,[†] Francesco Saverio Di Leva,[#] Sandro Cosconati,[∫] Luciana Marinelli,[#] Ettore Novellino,[#] Stuart F. J. Le Grice,[⊥] Angela Corona,[+] Yves Pommier,[ƒ] Christophe Marchand,[*,ƒ] and Roberto Di Santo[†]*

†Dipartimento di Chimica e Tecnologie del Farmaco, Istituto Pasteur-Fondazione Cenci Bolognetti, "Sapienza" Università di Roma, P.le Aldo Moro 5, I-00185, Roma, Italy

ƒLaboratory of Molecular Pharmacology, Center for Cancer Research, National Cancer Institute, National Institutes of Health, 37 Convent dr, Bethesda, MD 20892, USA

⊥RT Biochemistry Section, HIV Drug Resistance Program, National Cancer Institute, Frederick, MD 21702, USA

#Dipartimento di Farmacia, Università di Napoli "Federico II" Via D. Montesano 49, 80131 Napoli, Italy

∫DiSTABiF, Seconda Università di Napoli, Via Vivaldi 43, 81100 Caserta, Italy

+Department of Life and Environmental Sciences, University of Cagliari, Italy

Contents:

1. Spectroscopic data

3-Acetyl-1-[(4-fluorophenyl)methyl]-7-(piperazin-1-yl)quinolin-4(1*H*)-one (10a). Yellow solid; IR ν 2921 (NH), 1669 (C=O), 1653 (CO) cm^{-1}; ^1H NMR (DMSO-d_6) δ 2.63 (s, 3H, COCH_3), 3.30 (t, 4H, piperazine H), 3.46 (t, 4H, piperazine H), 5.64 (s, 2H, CH_2), 6.82 (d, 1H, quinolinone C8-H), 7.14-7.22 (m, 3H, quinolinone C6-H and benzene H), 7.36 (dd, 2H, benzene H), 8.10 (d, 1H, quinolinone C5-H), 8.75 (s, 1H, quinolinone C2-H).

3-Acetyl-1-[(4-fluorophenyl)methyl]-7-(4-methylpiperazin-1-yl)quinolin-4(1*H*)-one (10b). Yellow solid; IR ν 1661 (C=O) cm^{-1}; ^1H NMR (DMSO-d_6) δ 2.20 (s, 3H, N-CH_3), 2.38 (t, 4H, piperazine H), 2.63 (s, 3H, COCH_3), 3.26 (t, 4H, piperazine H), 5.63 (s, 2H, CH_2), 6.75 (d, 1H, quinolinone C8-H), 7.10 (dd, 1H, quinolinone C6-H), 7.19 (t, 2H, benzene H), 7.36 (dd, 2H, benzene H), 8.07 (d, 1H, quinolinone C5-H), 8.73 (s, 1H, quinolinone C2-H).

3-Ethyl-7-(4-ethylpiperazin-1-yl)-1-[(4-fluorophenyl)methyl]quinolin-4(1*H*)-one (10c). Yellow solid; IR ν 1661 (C=O), 1626 (C=O) cm^{-1}; ^1H NMR (DMSO-d_6) δ 1.14 (t, 3H, CH_2CH_3), 2.48 (q, 2H, CH_2CH_3), 2.57 (t, 4H, piperazine H), 2.83 (s, 3H, COCH_3), 3.25 (t, 4H, piperazine H), 5.32 (s, 2H, CH_2), 6.45 (d, 1H, quinolinone C8-H), 7.00-7.09 (m, 3H, quinolinone C6-H and benzene H), 7.18 (dd, 2H, benzene H), 8.35 (d, 1H, quinolinone C5-H), 8.54 (s, 1H, quinolinone C2-H).

3-Acetyl-7-(4-acetylpiperazin-1-yl)-1-[(4-fluorophenyl)methyl]quinolin-4(1*H*)-one (4d). Yellow solid; IR ν 1662 (C=O), 1639 (C=O), 1604 (C=O) cm^{-1}; ^1H NMR (DMSO-d_6) δ 2.04 (s, 3H, COCH_3), 2.63 (s, 3H, COCH_3), 3.32 (t, 4H, piperazine H), 3.54 (t, 4H, piperazine H), 5.64 (s, 2H, CH_2), 6.77 (d, 1H, quinolinone C8-H), 7.11 (dd, 1H, quinolinone C6-H), 7.20 (t, 2H, benzene H), 7.36 (dd, 2H, benzene H), 8.09 (d, 1H, quinolinone C5-H), 8.75 (s, 1H, quinolinone C2-H).

3-Acetyl-1-[(4-fluorophenyl)methyl]-7-thiomorpholinoquinolin-4(1*H*)-one (10e). Yellow solid; IR ν 1655 (C=O), 1637 (C=O) cm^{-1}; ^1H NMR ($CDCl_3$) δ 2.58 (m, 4H, thiomorpholine H), 2.83 (s, 3H, COCH_3), 3.67 (t, 4H, thiomorpholine H), 5.31 (s, 2H, CH_2), 6.39 (d, 1H, quinolinone C8-H), 6.94 (dd, 1H, quinolinone C6-H), 7.09 (t, 2H, benzene H), 7.19 (dd, 2H, benzene H), 8.35 (d, 1H, quinolinone C5-H), 8.55 (s, 1H, quinolinone C2-H).

3-Acetyl-1-[(4-fluorophenyl)methyl]-7-morpholinoquinolin-4(1*H*)-one (10f). Yellow solid; IR ν 1663 (C=O), 1630 (C=O) cm^{-1}; ^1H NMR ($CDCl_3$) δ 2.83 (s, 3H, COCH_3), 3.17 (m, 4H, morpholine H), 3.83 (t, 4H, morpholine H), 5.34 (s, 2H, CH_2), 6.46 (d, 1H, quinolinone C8-H), 7.01 (dd, 1H, quinolinone C6-H), 7.08 (t, 2H, benzene H), 7.19 (dd, 2H, benzene H), 8.38 (d, 1H, quinolinone C5-H), 8.57 (s, 1H, quinolinone C2-H).

3-Acetyl-7-(dimethylamino)-1-[(4-fluorophenyl)methyl]quinolin-4(1*H*)-one (10g). Yellow solid; IR ν 1660 (C=O), 1641 (C=O) cm^{-1}; ^1H NMR ($CDCl_3$) δ 2.63 (s, 3H, COCH_3), 2.95 (s, 6H, CH_3), 5.62 (s, 2H, CH_2), 6.44 (d, 1H, quinolinone C8-H), 6.87 (dd, 1H, quinolinone C6-H), 7.19 (t, 2H, benzene H), 7.35 (dd, 2H, benzene H), 8.06 (d, 1H, quinolinone C5-H), 8.74 (s, 1H, quinolinone C2-H).

3-Acetyl-1-[(4-fluorophenyl)methyl]-7-[4-(3-hydroxypropyl)piperazin-1-yl]quinolin-4(1*H*)-one (10h). White solid; IR ν 3423 (OH), 1649 (C=O), 1612 (C=O) cm^{-1}; ^1H NMR ($CDCl_3$) δ 1.74 (m, 2H, $OHCH_2CH_2CH_2N$), 2.58-2.64 (m, 6H, piperazine H and $OHCH_2CH_2CH_2N$), 2.79 (s, 3H, COCH_3), 3.19 (m, 4H, piperazine H), 3.80 (t, 2H, $OHCH_2CH_2CH_2N$), 5.27 (s, 2H, CH_2), 6.40 (d, 1H, quinolinone C8-H), 6.97 (dd, 1H, quinolinone C6-H), 7.04 (t, 2H, benzene H), 7.13 (dd, 2H, benzene H), 8.32 (d, 1H, quinolinone C5-H), 8.51 (s, 1H, quinolinone C2-H).

3-Acetyl-7-[4-(3-chloropropyl)piperazin-1-yl]-1-[(4-fluorophenyl)methyl]quinolin-4(1*H*)-one (10i). Yellow solid; IR ν 1656 (C=O), 1602 (C=O) cm^{-1}; ^1H NMR (DMF-d_7) δ 2.14 (m, 2H, $ClCH_2CH_2CH_2N$), 2.64-2.70 (m, 6H, piperazine H and $ClCH_2CH_2CH_2N$), 2.86 (s, 3H, COCH_3), 3.52

(m, 4H, piperazine H), 3.91 (t, 2H, Cl*CH*$_2$CH$_2$CH$_2$N), 5.95 (s, 2H, CH$_2$), 7.10 (d, 1H, quinolinone C8-H), 7.36 (dd, 1H, quinolinone C6-H), 7.43 (t, 2H, benzene H), 7.69 (dd, 2H, benzene H), 8.38 (d, 1H, quinolinone C5-H), 8.98 (s, 1H, quinolinone C2-H).

2. Table 1. Chemical and physical data of derivatives **8**, **9**, **10a-f** and **10h**.

Cpd	R7	mp (°C)	Recryst solvent[a]	Yield (%)
8 [b]	F	270-271	c	41
9 [b]	F	>300	b	29
10a	1-Pyperazinyl	231-232	d	32
10b	*N*-Methyl-1-Pyperazinyl	223-224	d	14
10c	*N*-Ethyl-1-Pyperazinyl	222-223	d	21
10d	*N*-Acethyl-1-Pyperazinyl	>300	d	52
10e	1-Thiomorpholinyl	221-222	g	52
10f	4-Morpholinyl	227-228	g	35
10g	*N,N*-Dimethylaminyl	dec.	c	52
10h	*N*-(3-Hydroxyprop-1-yl)-1-pyperazinlyl	230-231	d	78
10i	*N*-(3-Chloroprop-1-yl)-1-pyperazinlyl	192-193	d	48

[a] Recrystallization solvents: (a) aceton, (b) ethanol, (c) isopropanol, (d) toluene, (e) toluene/cyclohexane, (f) benzene/cyclohexane, (g) benzene, (h) methanol; [b] Reference[19b]

3. Analyses

Compd	Elemental Analyses Calculated/ Found					
	C	H	N	Cl	F	S
11a	65.13	5.47	8.76		3.96	
	65.29	5.67	8.70		3.92	
11b	65.71	5.72	8.51		3.85	
	66.01	5.87	8.31		3.80	
11c	66.26	5.96	8.28		3.74	
	66.35	5.86	7.95		3.82	
11d	64.48	5.41	8.06		3.64	

	64.20	5.25	8.39		3.69	
11e	62.89	5.07	5.64		3.83	6.46
	62.78	5.21	5.71		3.82	6.44
11f	64.99	5.24	5.83		3.95	
	64.73	4.99	5.70		3.91	
11g	65.74	5.29	6.39		4.33	
	65.61	4.93	6.60		4.51	
11i	62.64	5.62	7.56	6.38	3.42	
	62.65	5.78	7.87	6.40	3.55	
12a	63.85	4.91	9.31		4.21	
	63.50	5.20	8.99		4.19	
12b	64.51	5.20	9.03		4.08	
	64.51	5.25	9.03		4.30	
12c	65.13	5.47	8.76		3.96	
	65.50	5.34	8.61		4.11	
12d	63.28	4.90	8.51		3.85	
	63.59	4.98	8.68		3.80	
12e	61.53	4.52	5.98		4.06	6.84
	61.55	4.48	5.96		3.97	6.88
12f	63.71	4.68	6.19		4.20	
	63.69	4.53	6.18		4.22	
12g	64.39	4.67	6.83		4.63	
	64.40	4.39	7.01		4.50	
12i	61.42	5.15	7.96	6.71	3.60	
	61.49	5.21	8.18	6.75	3.66	

4. Molecular Modelling

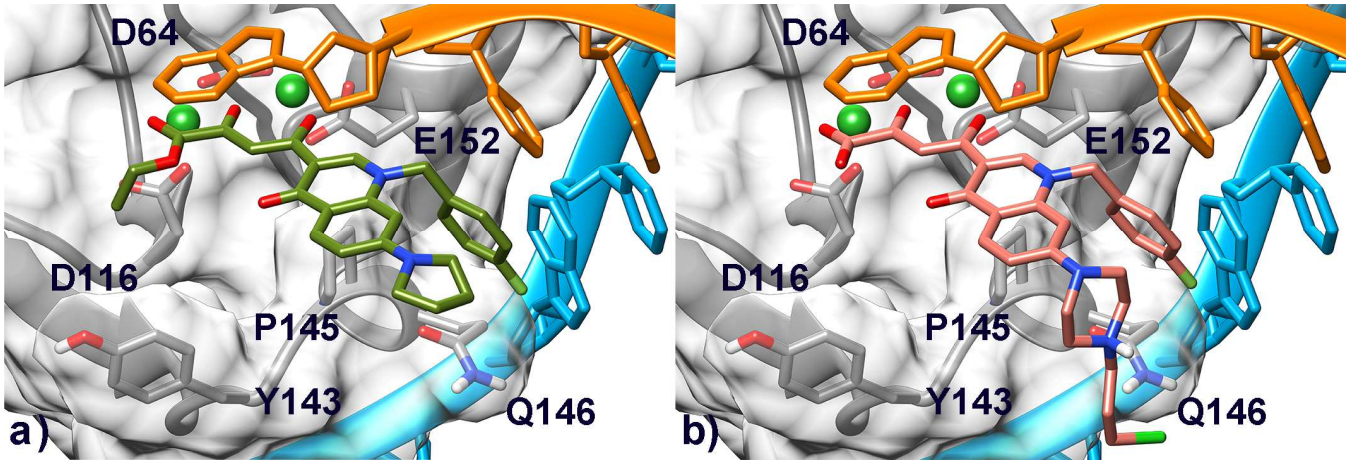

Figure S1. a) Binding modes of compound **7a** (green sticks) and **12i** (pink sticks) within the HIV-1 IN/DNA model. The CCD is depicted as transparent light gray surface and ribbons. Amino acid side chains involved in ligand binding are represented as sticks. The non-cleaved (cyan) and processed (orange) viral DNA strands are shown as ribbon and sticks. Mg^{2+} metal ions are represented as green spheres.

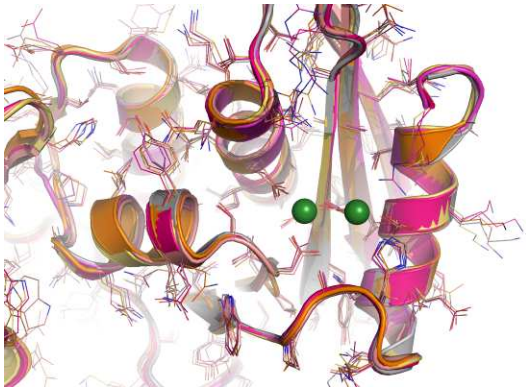

Figure S2. Superposition of all of the available crystal structures of the full-length wild-type RT or the isolated RNase H CCD from HIV-1 in complex with RNase H inhibitors on the alpha carbon atoms. All of the structures are represented as cartoons and lines. PDB codes are: 3K2P (fuchsia), 3QIP (pink), 3IG1 (orange), 3LP0 (magenta), 3LP1 (yellow), 3LP3 (gray). Such a superimposition shows that the protein folding, the loops shape and the side chain conformations of the majority of the residues within the catalytic site are highly conserved. The picture was rendered with PyMol 0.99rc6.

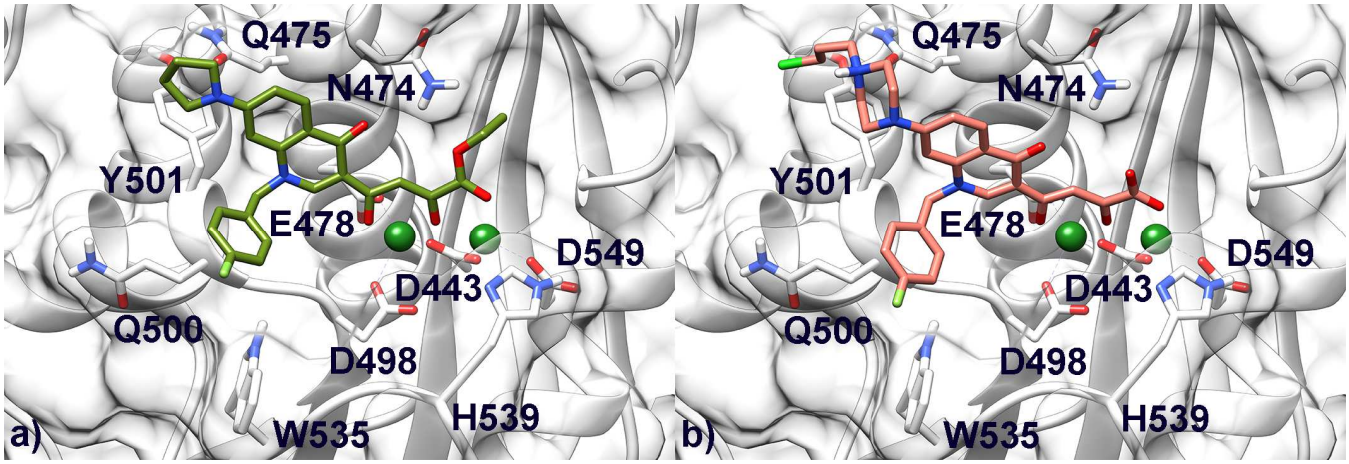

Figure S3. Binding mode of compound **7a** (green sticks) and **12i** (pink sticks) in the HIV-1 RNase H active site. The enzyme is shown as transparent white surface and ribbons. Amino acid side chains important for ligand binding are represented as sticks. Mg^{2+} metal ions are depicted as green spheres.

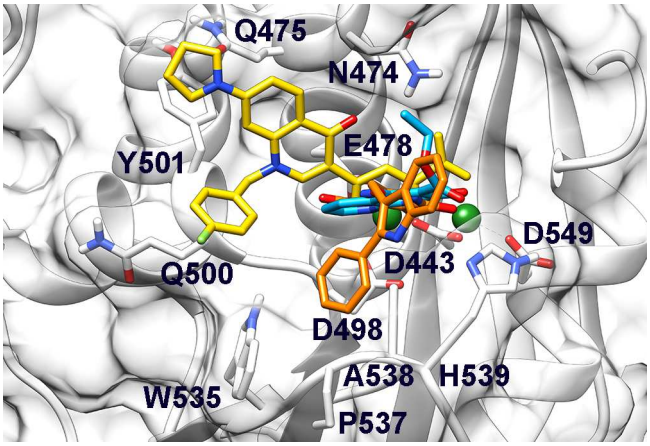

Figure S4. Comparison between the binding modes of **7b** (yellow) and a naphthyridinone (orange) and a pyrimidinol carboxylic acid co-crystallized with the HIV-1 RT enzyme at the RNase H active site (PDB codes 3LP0[1] and 3QIP[2]). The active site is shown as transparent white surface and ribbons. Amino acid side chains important for ligand binding are represented as sticks. Mg^{2+} metal ions are depicted as green spheres.

References

(1) Su, H.-P.; Yan, Y.; Prasad, G. S.; Smith, R. F.; Daniels, C. L.; Abeywickrema, P. D.; Reid, J. C.; Loughran, H. M.; Kornienko, M.; Sharma, S.; Grobler, J. A.; Xu, B.; Sardana, V.; Allison, T. J.; Williams, P. D.; Darke, P. L.; Hazuda, D. J.; Munshi, S. Structural basis for the inhibition of RNase H activity of HIV-1 reverse transcriptase by RNase H active site-directed inhibitors. *J. Virol.* **2010**, *84*, 7625–7633.

(2) Lansdon, E. B.; Liu, Q.; Leavitt, S. A.; Balakrishnan, M.; Perry, J. K.; Lancaster-Moyer, C.; Kutty, N.; Liu, X.; Squires, N. H.; Watkins, W. J.; Kirschberg, T. A. Structural and binding analysis of pyrimidinol carboxylic acid and N-hydroxyquinazolinedione HIV-1 RNase H inhibitors. *Antimicrob. Agents Chemother.* **2011**, *55*, 2905–2915.